

Cave-adapted evolution in the North American amblyopsid fishes inferred using phylogenomics and geometric morphometrics

Pamela B. Hart,^{1,2}  Matthew L. Niemiller,³  Edward D. Burress,⁴  Jonathan W. Armbruster,⁵ 
 William B. Ludt,⁶  and Prosanta Chakrabarty¹ 

¹Museum of Natural Sciences and Department of Biological Sciences, Louisiana State University, Baton Rouge, Louisiana 70803

²E-mail: pamelabeth.hart@gmail.com

³Department of Biological Sciences, The University of Alabama in Huntsville, Huntsville, Alabama 35899

⁴Department of Evolution and Ecology, University of California, Davis, California 95616

⁵Museum of Natural History and Department of Biological Sciences, Auburn University, Auburn, Alabama 36830

⁶Department of Ichthyology, Natural History Museum of Los Angeles County, Los Angeles, California 9007

Received August 24, 2019

Accepted February 27, 2020

Cave adaptation has evolved repeatedly across the Tree of Life, famously leading to pigmentation and eye degeneration and loss, yet its macroevolutionary implications remain poorly understood. We use the North American amblyopsid fishes, a family spanning a wide degree of cave adaptation, to examine the impact of cave specialization on the modes and tempo of evolution. We reconstruct evolutionary relationships using ultraconserved element loci, estimate the ancestral histories of eye-state, and examine the impact of cave adaptation on body shape evolution. Our phylogenomic analyses provide a well-supported hypothesis for amblyopsid evolutionary relationships. The obligate blind cavefishes form a clade and the cave-facultative eyed spring cavefishes are nested within the obligate cavefishes. Using ancestral state reconstruction, we find support for at least two independent subterranean colonization events within the Amblyopsidae. Eyed and blind fishes have different body shapes, but not different rates of body shape evolution. North American amblyopsids highlight the complex nature of cave-adaptive evolution and the necessity to include multiple lines of evidence to uncover the underlying processes involved in the loss of complex traits.

KEY WORDS: Ancestral state reconstruction, cavefishes, geometric morphometrics, phylogenomics, regressive evolution, ultra-conserved elements.

Convergent evolution is a fascinating natural phenomenon where multiple lineages independently evolve similar phenotypes in response to selection pressures imposed by the ecosystem (Conway Morris 2010; Losos 2011). Many of the most dramatic examples of convergent evolution have occurred in extreme and/or geographically isolated ecosystems and include the deep sea, river channels, islands, deserts, mountain tops, and caves (Azua-Bustos et al. 2012; Alter et al. 2015; Page and Cooper 2017; Martinez et al. 2018). In particular, these ecosystems impose harsh physiological demands upon resident organisms. Morphologi-

cal convergence can include complex traits such as coloration, metabolism, and sensory processes (Passow et al. 2015; Passow et al. 2017; Martinez et al. 2018). Such complex traits were once thought to be integral to the success and longevity of an organism; however, these traits can diminish or even disappear in extreme environments. Examples of complex traits that have been convergently lost include limbs in aquatic mammals (Berta et al. 2006) and eye structures/visual systems in many cave-obligate organisms (Trontelj et al. 2012; Soares and Niemiller 2020).

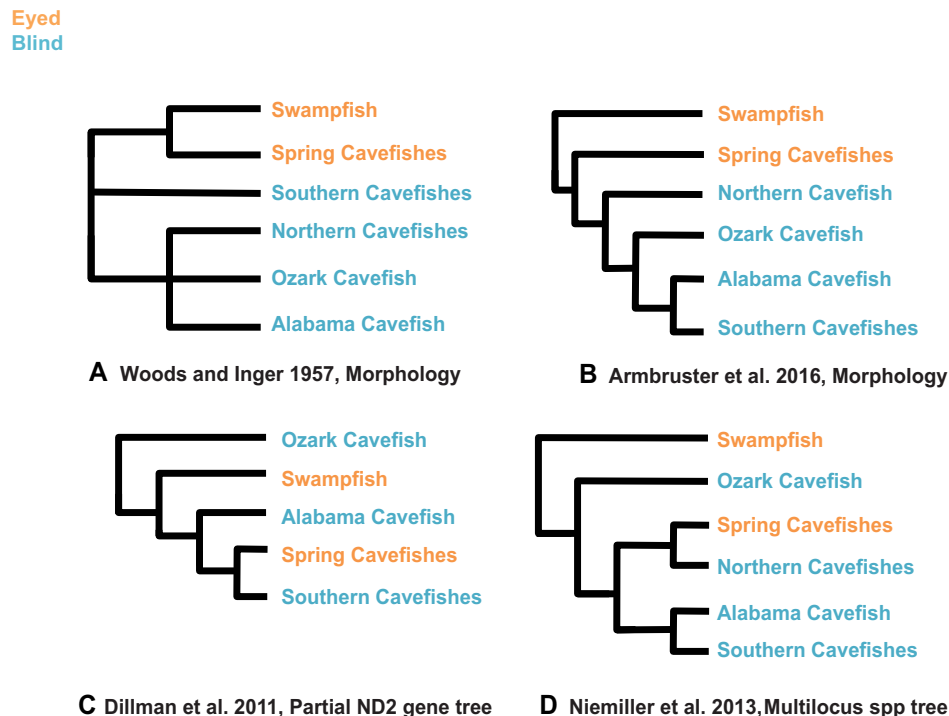


Figure 1. Previous conflicting phylogenetic relationships of the Amblyopsidae using both morphological (A and B) and molecular (C and D) datasets. Eyed fishes = orange; blind fishes = blue.

A lasting topic in evolutionary biology has been the reversibility of complex trait loss. Dollo's Law states that once a complex trait (e.g., limbs or eyes) has been lost, it cannot then be regained (Dollo 1893). Yet, with the wide use of molecular methods and ancestral state reconstructions, challenges to the Law of Irreversibility have surfaced in recent years, such as snail shell coiling (Collin and Cipriani 2003), Crotoniidae mite sexuality (Domes et al. 2007), oviparity in snakes (Lynch and Wagner 2009), salamander metamorphosis (Bonett et al. 2013), and eye redevelopment (Oakley and Cunningham 2002).

An excellent group to study both convergent evolution as well as the Law of Irreversibility are the Amblyopsidae fishes from North America. This family includes closely related surface-dwelling species that have well-developed, functional eyes and cave-dwelling species that lack external eye characters and visual perception (Woods and Inger 1957; Poulson 1963; Poulson and Niemiller 2010; Armbruster et al. 2016). The most recent and complete dated molecular phylogenetic investigation recovered the eyed spring cavefishes nested within the larger group of blind cavefishes (Niemiller et al. 2013). The recovery of eyed fishes within a blind group raises the discussion of ancestral character state for these fishes. If the ancestor to these fishes was blind, this could indicate a reversal in eye state leading to the eyed spring cavefishes. Additional molecular and morphological investigations have resulted in conflicting phylogenetic hypotheses (Fig. 1; Woods and Inger 1957; Dillman et al. 2011;

Armbruster et al. 2016), such as multiple independent cave invasions and convergence on eye-loss rather than reversing eye state.

Morphological work supports an evolutionary transition from the eyed Swampfish (*Chologaster cornuta*) to the smaller-eyed spring cavefishes (*Forbesichthys* spp.) to the blind cavefishes (*Amblyopsis*, *Troglichthys*, *Typhlichthys*, and *Speoptatyrhinus*), also known as the morphological continuum hypothesis or progressive regressionism (Figs. 1A and 1B; Woods and Inger 1957; Romero and Green 2005; Armbruster et al. 2016). These relationships suggest an eyed, pigmented ancestor for the Amblyopsidae and a single ancestor that gave rise to all cave-obligate species, which converged upon similar cave-adapted phenotypes.

Conversely, molecular analyses indicate the presence of one or both of the eyed genera nested within cave-obligate groups (Figs. 1C and 1D). This particular result suggests one of two scenarios: (1) the eyed spring cavefishes re-evolved or redeveloped eyes or (2) that eyes were lost at least three times (one per major cavefish lineage). Ancestral state reconstruction of eyes (functional vs. degenerate) and model testing on the most complete amblyopsid phylogeny by Niemiller et al. (2013) supports a blind, depigmented ancestor to the eyed spring cavefishes + blind cavefishes clade (Fig. 1D). The most likely scenario out of those tested was a single subterranean invasion followed by cave adaptation. Then, this cave-obligate ancestor

dispersed and speciated into multiple cave-obligate lineages, but with a single lineage recolonizing the surface habitat and either re-evolving or redeveloping functional eyes (i.e., the eyed spring cavefishes).

However, re-evolution of complex traits (e.g., eyes) is in direct contrast to Dollo's Law of Irreversibility (Dollo 1893) and the morphological continuum hypothesis (Woods and Inger 1957). Further, eye histology as well as differences in *rhodopsin* eye gene mutations indicate eye structure loss in different ways in each cavefish lineage, suggesting independent mechanisms for loss in each cave lineage (i.e., convergence; Eigenmann, 1897, 1909; Niemiller and Poulson 2010; Niemiller et al. 2013). As additional support for the convergence scenario, Armbruster et al. (2016) stress in the most recent morphological phylogenetic investigation that although they find support for progressive regressionism, there are few synapomorphies for internal nodes in the phylogeny. The authors also note that the morphological similarities seen in cave-adapted species across multiple clades could be due to convergence instead of common descent (Armbruster et al. 2016). Convergence on reductive traits in cave animals is apparent with pale forms devoid of pigment, the elongation of limbs, and loss of eyes (Poulson 1963; Hedin and Thomas 2009; Christiansen 2012; Pipan and Culver 2012; Trontelj et al. 2012; Soares and Niemiller, 2013, 2020). Additional morphological convergence, such as body shape convergence (e.g., dorsoventral head-flattening and a duck-bill-like rostral flaring), has been noted in cave-obligate vertebrates ranging from fishes to salamanders, but has not yet been quantified (Christiansen 2012; Fenolio et al. 2013; Edgington and Taylor 2019; Soares and Niemiller 2020).

To evaluate the alternate hypotheses that cave-adapted species arose from a single cave-adapted ancestor or independently converged on similar cave-adapted phenotypes, we employed phylogenomic, morphometric, and phylogenetic comparative methods. We reconstructed the evolutionary relationships among amblyopsids with ultraconserved element (UCE) loci using maximum likelihood (ML) and coalescent species tree estimation methods. Second, we estimated the ancestral state history of eye state (eyed and blind) for the Amblyopsidae. Third, we quantified body shape with landmark-based geometric morphometrics (GM) and compared rates of morphological evolution between eye states. Our major goals were (1) to clarify uncertainty in the evolutionary relationships among amblyopsids by employing a phylogenomic dataset, (2) resolve competing hypotheses about the evolutionary history of cave-colonization by this group (i.e., progressive regressionism, singular cave invasion with eye redevelopment in the spring cavefishes, or multiple cave invasions), and (3) assess the impact of cave-adaptation on patterns of body shape evolution.

Materials and Methods

STUDY GROUP

The amblyopsid fishes are found across the Eastern and Southeastern United States, ranging from the Ozarks to the Atlantic Coast (Fig. 2; Niemiller and Poulson 2010). The Amblyopsidae have been recovered within the order Percopsiformes with both morphological and molecular data (Springer and Johnson 2004; Near et al. 2012; Betancur-R. et al. 2013; Niemiller et al. 2013; Armbruster et al. 2016). There are six genera that comprise the family that exhibit varying degrees of troglomorphy (i.e., morphological, physiological, and behavioral traits associated with cave inhabitation; Table 1): the surface eyed Swampfish (*Chologaster cornuta*), the facultative cave-dwelling eyed spring cavefishes (i.e., *Forbesichthys agassizii* and *F. papilliferus*), and the blind cave-obligate cavefishes (*Amblyopsis spelaea*, *A. hoosieri*, *Speoplatyrhinus poulsoni*, *Troglichthys rosae*, and *Typhlichthys eigenmanni* and *Ty. subterraneus*). All specimens collected for this study were deposited in museum collections for future study following guidelines and permissions from permitting agencies (Tables S1–S3; IACUC Protocol 19–091).

PHYLOGENOMICS

We collected specimens or obtained tissue and specimen loans for all genera of the Amblyopsidae ($N = 110$; Table S1). The outgroup consisted of other percopsiform fishes, including the Trout Perch (*Percopsis omiscomaycus*; $N = 1$) and Pirate Perch (*Aphredoderus sayanus*; $N = 1$). We used a reduced representation genomic dataset of UCE loci to reconstruct the amblyopsid phylogeny. UCE loci are molecular markers in animal genomes that are conserved across the Tree of Life (Faircloth et al. 2012). Their highly conserved nature allows for comparison across species, whereas variable flanking regions can be used to identify diversity. All genetic data have been submitted to GenBank (Table S1). Of note is the extensive sampling for the Southern Cavefish (*Ty. subterraneus*): as the largest ranging cavefish in the world and also representing a species complex (Niemiller et al. 2012, 2016), the Southern Cavefish has been more highly sampled than the other members of the family.

Molecular labwork

We extracted whole genomic DNA via EZNA (Omega Biotek, Norcross, GA, 30071) and DNeasy Blood and Tissue (Qiagen, Germantown, MD, 20874) kits from fin clips stored in 95% ethanol or RNA Later. Genomic DNA was quantified using a Qubit 2.0 fluorometer. Random shearing of the extracted DNA to ~600 bp was performed using an Episonic Multi-Functional Bioprocessor. We performed target capture of 1300 UCE loci using the HyperPrep Kit for library

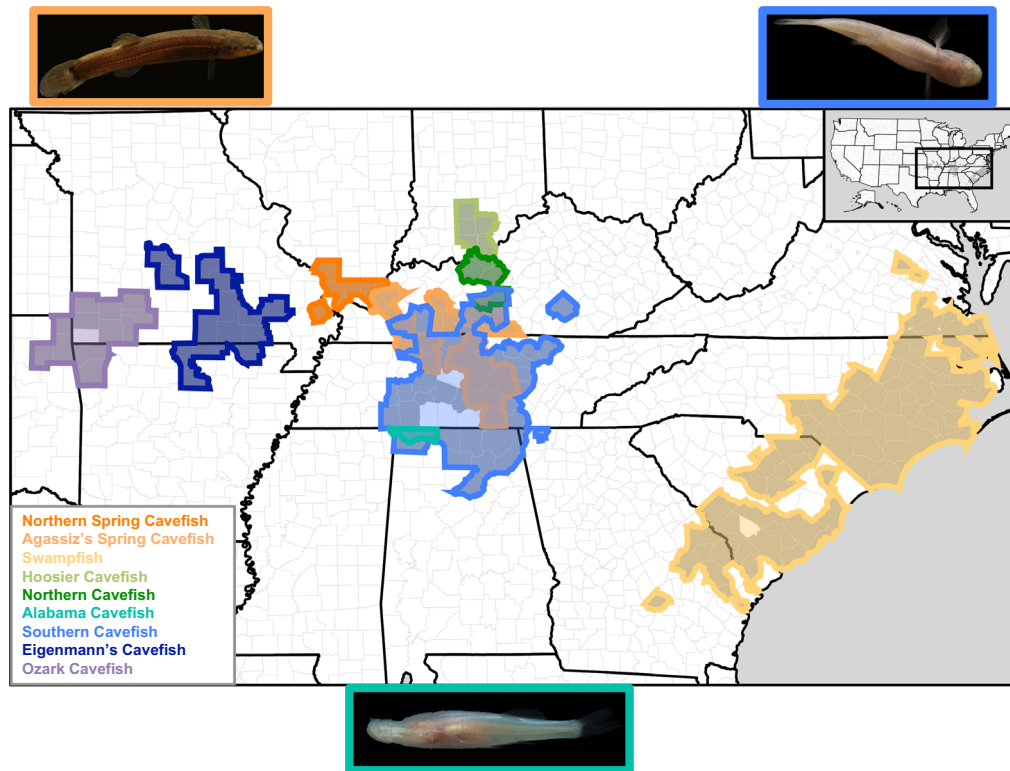


Figure 2. Amblyopsid distribution across the continental United States. Dark filled counties are counties with records; light unfilled counties do not have any records. Sympatry and syntopy occur in Kentucky, Tennessee, and Alabama. Interestingly, sympatry occurs only between nonsister species.

Table 1. All species of the Amblyopsidae with associated common names and species descriptions.

Common name	Genus	Species	Descriptor
Northern Cavefish	<i>Amblyopsis</i>	<i>spelaea</i>	DeKay 1842
Hoosier Cavefish	<i>Amblyopsis</i>	<i>hoosieri</i>	Chakrabarty et al. 2014
Swampfish	<i>Chologaster</i>	<i>cornuta</i>	Agassiz 1853
Northern Spring Cavefish	<i>Forbesichthys</i>	<i>papilliferus</i>	Forbes 1882; resurrected in Niemiller et al. 2013; valid in Chakrabarty et al. 2014; Armbruster et al. 2016; Burress et al. 2017
Agassiz's Spring Cavefish	<i>Forbesichthys</i>	<i>agassizii</i>	Putnam 1872
Alabama Cavefish	<i>Speoplatyrhinus</i>	<i>poulsoni</i>	Cooper and Kuehne 1974
Ozark Cavefish	<i>Troglichthys</i>	<i>rosae</i>	Eigenmann 1898
Southern Cavefish	<i>Typhlichthys</i>	<i>subterraneus</i>	Girard 1859
Eigenmann's Cavefish	<i>Typhlichthys</i>	<i>eigenmanni</i>	Charlton 1933; valid in Niemiller et al. 2013; Chakrabarty et al. 2014

preparation and the MYbaits UCE Acanthomorph target capture kit (1341 UCE loci, 2600 probes, Arbor Biosciences, Ann Arbor, MI, 48103; McGee et al. 2016) following manufacturer protocols with all reaction quantities scaled by half. Sequencing was completed on the Illumina HiSeq300-PE150 platform at the Oklahoma Medical Research Foundation with $\sim 30\times$ sequencing coverage.

Bioinformatics processing and phylogenetic analyses

We cleaned reads with the *illumiprocessor* function from the Phyluce (version 1.5) pipeline using *trimmomatic* (Phyluce: Faircloth et al., 2012, 2013, 2016; Trimmomatic: Bolger et al. 2014). We assembled reads using the ABySS assembler (version 1.9.0; Simpson et al. 2009) on the Louisiana State University High Performance Computing cluster SuperMike-II. We used a kmer

value of 55 for the ABySS assembly. We extracted UCE contigs (commands *phyluce_assembly_match_contigs_to_probes*, *phyluce_assembly_get_match_counts*, and *phyluce_assembly_get_fastas_from_match_counts*) and aligned the UCE loci (*phyluce_align_seqcap_align*) using the Phyluce pipeline. A data matrix with 75% completeness was created with *phyluce_align_get_only_loci_with_min_taxa*. We used Partition-Finder2 on XSEDE (version 2.1.1; Lanfear et al. 2017) on the CIPRES Science Gateway (version 3.3; <https://www.phylo.org/>) to group similar data blocks of the full UCE loci, estimating the best partitioning scheme with the best model of sequence evolution while ensuring we are not over-partitioning.

We used RAxML-HPC2 on XSEDE (version 8.2.10; Stamatakis 2014) on CIPRES Science Gateway (version 3.3; <https://www.phylo.org/>) for ML phylogenetic reconstruction with the GTRCAT sequence model of evolution. For coalescent species tree analysis, we used SVDQuartets in PAUP* (version 4.0a; PAUP*: Swofford 2002; SVDQuartets: Chifman and Kubatko 2014). Additionally for coalescent analysis, we used ASTRAL-II (version 4.1.1, Mirarab and Warnow 2015). ASTRAL-II takes into account gene tree incongruence by using gene trees as input. Gene trees and bootstraps for ASTRAL-II were generated in RAxML (version 8.2.11) on the Louisiana State University High Performance Computing Cluster Super-Mike and then inputted into ASTRAL-II.

For all subsequent comparative analyses, we used the 75% complete data-matrix ASTRAL-II coalescent species tree. The tree was rooted using the Troutperch (*Percopsis omiscomaycus*) in FigTree (version 1.4.2). We transformed the tree to be ultrametric (i.e., relative times) using the *chronopl* function implemented in the R package *ape* (version 3.2; Paradis et al. 2004).

Historical introgression, hybridization, incomplete lineage sorting, and recombination are a few biological possibilities that may result in nonbifurcating relationships (Huson and Scornavacca 2011). Phylogenetic trees do not show relationships other than those that are bifurcating (Huson and Bryant 2006; Morrison 2011); however, phylogenetic networks such as data display and evolutionary networks can be used to examine nontree-like relationships (Huson and Bryant 2006; Huson and Scornavacca 2011; Morrison 2011). Sympatry within the family naturally brings up questions about hybridization and introgression (Fig. 2). The extent to which hybridization occurs among the amblyopsids is unknown. It is possible that the eyed spring cavefishes are the product of hybridization between eyed surface fishes and blind cavefishes. Additionally, the connectivity and hybridization potential for the sympatric blind fishes is also unknown. To examine if there were nontree-like relationships within the Amblyopsidae, we created a splits network using SplitsTree4 (version 4.15.1; Huson and Bryant

2006). A Neighbor-Net splits network was created using uncorrected P-distances estimated from sequence data for all individuals ($N = 110$). We then visualized the splits network using the Rooted Equal Angle algorithm (Gambette and Huson 2008).

ANCESTRAL STATE RECONSTRUCTION

We estimated the evolutionary history of eye state (eyed and blind) using two methods. We first used a Bayesian framework implemented in RevBayes (Höhna et al. 2016). In this procedure, we used reversible jump Markov chain Monte Carlo (MCMC) to test the probability that the transition rate from blind to eyed was zero (i.e., irreversibility). We specified two fixed priors. We assumed a transition rate for the exponential prior distribution as the length of the tree divided by two. Two is an appropriate prior for the number of transitions as it equally pertains to each of the opposing hypotheses (two independent transitions to blind or a single transition to blind followed by a second transition to eyed). Second, we specified the a priori probability of 0.5 that a rate is equal to 0. Rate variables for each transition were drawn from identical exponential distributions based on the rate prior. The reversible jump distributions draw either a constant value (zero in this case—meaning no transition rate) or draw a rate from the base exponential distribution. We calculated the posterior probability of a transition rate of zero by comparing the frequency with which a rate of zero is sampled. Because the rates are drawn independently, the eyed-to-blind and blind-to-eyed transition rates can be different. The estimation of root state frequencies can lead to erroneous interpretation (Goldberg and Igić 2008); therefore, we draw these values from a Dirichlet distribution rather than use fixed values. The MCMC was run for 10k generations with two independent runs. The models we tested using the Bayesian method were equal rates (mK), free rate change (freeK), and irreversibility (that eyes can be lost but not regained; i.e., Dollo's Law). We also used the *make.simmap* (Bollback 2006) function implemented in the R package *phytools* (version 0.4-56; Revell 2012) to perform stochastic character mapping. The ancestral states of the internal nodes were summarized across 1000 stochastic character histories. We compared results assuming equal transition rates (ER), different transition rates (ARD), as well as irreversibility. We performed these analyses on a pruned version of our ASTRAL-II species tree. We included a single individual per locality except for localities that were polyphyletic ($N = 86$; Table S1).

GEOMETRIC MORPHOMETRICS

We performed landmark-based GM on the lateral left-hand view of two-dimensional and radiograph images of museum specimens. Previous literature found a significant correlation between age and body shape in the Southern Cavefish (Burress et al.

2017); thus, we restricted our dataset to adult specimens to reduce the influence of ontogenetic allometry in our analyses. Our landmarks consisted of static, sliding, and unbend landmarks and these were digitized using *tpsDig* (Fig. S1 and Supporting Information Material 3; Rohlf 2010). The *unbend* function in *tpsUtil* was used to remove curvature of the specimen caused by preservation. This function fits the user-specified points to a quadratic curve, effectively removing artificial curvature. The *unbend* landmarks were then removed after the function was applied.

We then used the package *geomorph* (version 3.1.1; Adams and Otárola-Castillo 2013; Adams et al. 2019) in RStudio (version 1.2.1335; RStudio, Inc.) to perform further analyses. The *.tps* file was read into *geomorph* via the *readland.tps* function. Semi-landmarks were designated using the function *define.sliders.2d*. We then performed a Generalized Procrustes Analysis (GPA) using the *gpagen* function with the Procrustes Distance criterion to optimize sliding landmark position during GPA. GPA is used to obtain shape variables from landmark data. GPA removes information unrelated to shape by translating the landmark configurations to the origin, scaling to unit-centroid size, and rotating the configurations using an optimality criterion such that the sum of squared distances between corresponding landmarks is minimized (i.e., least-squares criterion on Procrustes distances; Gower 1975; Klingenberg 2016).

Full GM dataset

There was a total of 146 individuals from four amblyopsid genera in our full GM dataset (Table S2). To assess major axes of body shape diversity among amblyopsids, we generated principal components (PCs) on the covariance matrix generated from the generalized Procrustes analysis using the *plotTangentSpace* function in *geomorph*, which automatically removes axes with zero variance. We then visualized morphospace by delineating eye state on biplots of PC scores.

We determined if there were statistically significant differences in shape between eye-states using all PCs with nonzero variance using the base *manova* function in R. We were unable to incorporate phylogeny with our full GM dataset because there were not corresponding tips for all specimens; however, we incorporated phylogeny into analyses based on a subset of specimens ($N = 18$; see next section).

GM voucher sample dataset

We created a *.tps* file and performed GPA using the *gpagen* function on a subset of voucher specimens that matched our ASTRAL-II coalescent species tree either identically (blind cavefishes) or matched in locality such that we were confident they depicted the same population (eyed spring cavefishes and Swampfish; $N = 18$; Table S3). We treated populations/locality as our primary unit of replication, rather than species, because

of known but undescribed cryptic lineage diversity in both the Southern Cavefish and Eigenmann's Cavefish (Niemiller et al. 2012). For the blind cavefishes, we used only voucher specimens in which there were matches between molecular and morphological data due to evidence that some caves are not monophyletic and therefore not representative of populations (Figs. S2–S4).

We used this voucher subset to test and account for shared evolutionary history in our body shape analyses. First, we tested for phylogenetic signal in our shape data with the function *physignal* (Blomberg et al. 2003; Adams 2014a); this command uses Procrustes shape data to estimate the degree of phylogenetic signal in a dataset. Phylogenetic signal is evaluated relative to Brownian motion using the generalized K-statistic (Blomberg et al. 2003) that has been adapted for high-dimensional multivariate datasets (Adams 2014a). Significance is evaluated by permutations of the shape data across the tips of the phylogeny (Adams et al. 2019). We then performed Principal Components Analysis (PCA; *plotTangentSpace*) on the Procrustes shape data to visualize the axes of greatest shape variation. To understand the direction and magnitudes of shape changes along branches of the phylogeny, we created a GM phylomorphospace (Sidlauskas 2008) using the *geomorph* function *plotGMphylomorphospace* on the Procrustes coordinates.

Next, we performed a phylogenetic Multivariate Analysis of Variance (MANOVA) using *procD.pgls* using the Procrustes coordinates as input to account for all of shape space. We used phylogenetic MANOVA to determine if there were significant differences in body shape between eye states while accounting for phylogeny in a multivariate framework. The model was run for 1000 iterations.

We tested for and quantified morphological convergence among the cavefishes using the distance-based method devised by Stayton (2015). This method was constructed on the idea that two taxa evolving in a convergent manner will be more similar morphologically to one another than their ancestors were to each other; this test was implemented with the package *convevol* (version 1.3; Stayton 2015) in RStudio. We performed *convrat* followed by *convratsig* to estimate four values of convergence and the significance values of the convergence estimates, respectively. The *convrat* function first calculates the Euclidian phenotypic distance between two taxa. *Convrat* then calculates maximum phenotypic distance between two lineages from the most recent common ancestor to the tips using ancestral state reconstruction under a Brownian motion model. The total amount of phenotypic evolution in a clade (based on the most recent common ancestor) is estimated. Last, the function also evaluates the total amount of phenotypic evolution in the given tree. Significance testing for the convergence statistics estimated by *convrat* is performed through evolutionary simulations using the *convrat-sig* function (Stayton 2015). For these methods, we used the first

four PCs meeting the statistical criteria for fewer shape variables than putatively convergent taxa (Page and Cooper 2017). *Convevol* provides four measures of convergence: C1 is an index of convergence that does not take into account the absolute amount of evolution during convergence (i.e., if there is a large or small phenotypic difference between the convergent taxa; value from 0 to 1), C2 builds upon the convergence index by taking the magnitude of change into account within the dataset, and C3 and C4 permit comparisons between datasets (Stayton 2015). C1 through C4 are calculated for each possible pair of taxa and then averaged. We performed 1000 iterations for significance testing.

Last, we compared the rates of morphological evolution between eye states. We estimated and compared evolutionary rates via the *compare.evol.rates* function (Adams 2014b; Denton and Adams 2015; Adams and Collyer 2018) in geomorph using the Generalized Procrustes coordinates as input. This function estimates and compares the net rates of morphological evolution for two or more groups of species in a phylogenetic tree evolving under Brownian motion. We estimated significance by performing 999 iterations.

Results

PHYLOGENOMICS

The 75% complete data matrix was composed of 897 UCE loci. The minimum number of unique contigs for an individual captured was 655 and the maximum was 987 with an average of 918.6 contigs. We sampled all six amblyopsid genera with multiple individuals per species except for the federally endangered Alabama Cavefish (*S. poulsoni*) for a total of 110 samples (Table S1).

Phylogenetic trees

The ML reconstruction recovered both eyed amblyopsids as sister taxa to blind cavefishes (Figs. 3 and Fig. S2). This topology is novel among all existing phylogenetic hypotheses for amblyopsids. The most surprising result is the sister group relationship of the blind Ozark Cavefish and eyed Swampfish; however, this topology is not supported by our other phylogenomic reconstructions. Additionally, although we have high bootstrap support for this topology, we acknowledge that bootstrap support can be inflated with such large datasets and that long-branch attraction is a substantial problem in this analysis (Felsenstein 1978; Huelsenbeck 1997; Bergsten 2005).

The ASTRAL-II topology was identical to that recovered in Niemiller et al. (2013) in that we recovered the eyed spring cavefishes (*Forbesichthys* spp.) as the sister group to the blind *Amblyopsis* spp. cavefishes, nesting the spring cavefishes within cave-obligate taxa (Fig. 4A and Fig. S3). We recovered the eyed Swampfish as the sister group to the rest of the amblyopsids.

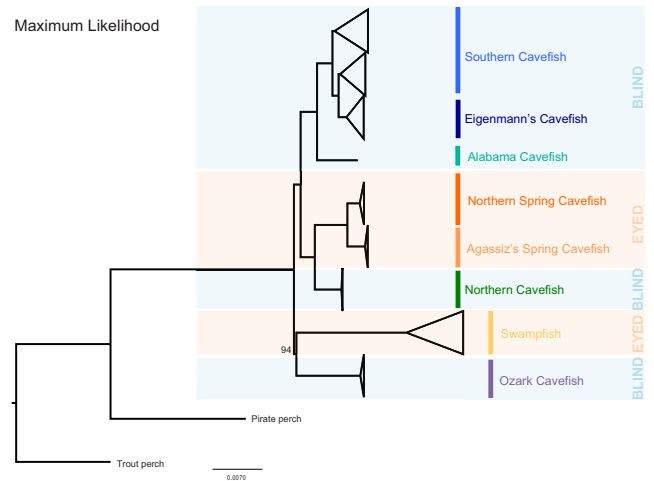


Figure 3. Amblyopsidae UCE RAxML phylogenomic tree created with 75% complete data matrix. Colored boxes indicate the extant taxa eye-state. Bootstrap node values are 100 unless otherwise noted. Scale bars indicate expected number of substitutions. Cool-colored species are blind (Northern Cavefish = green; Southern Cavefish = light blue; Eigenmann's Cavefish = dark blue; Alabama Cavefish = aquamarine; Ozark Cavefish = purple) and warm-colored species are eyed (Agassiz's Spring Cavefish = light orange; Northern Spring Cavefish = dark orange; Swampfish = yellow).

The SVDQuartets topology matched the ASTRAL-II topology with slightly differing support values (Fig. 4B and Fig. S4): the eyed spring cavefishes (*Forbesichthys* spp.) are the sister group to the blind *Amblyopsis* cavefishes and the eyed Swampfish are the sister group to the rest of the family.

Splits network

Our splits network shows many reticulate events and evidence for nontree-like relationships within the amblyopsids (Fig. 6). The most co-ancestry and nontree-like relationships occur within the blind cavefish genus *Typhlichthys*. Reticulate events do appear between the eyed spring cavefishes and the blind Northern Cavefish. Reticulate events also appear between the blind Ozark Cavefish and the eyed Swampfish (Fig. 5).

ANCESTRAL STATE RECONSTRUCTION

The lowest supported models in our Bayesian reconstruction were the mK model (Akaike Information Criterion = 36.27; Fig. 6A) and the freeK model (AIC = 31.16; Fig. 6B) The most highly supported model was the Irreversibility model (AIC = 30.13; Fig. 6C). In the Irreversibility model, we found high support for eyed ancestral states for the blind cavefishes (Fig. 6C, nodes I and II).

The ER model was the least supported model from the stochastic character mapping (AIC = 35.23; Fig. S5A). Our ARD was second most supported model and our Irreversibility model was the most highly supported (AIC = 26.08 and 25.06,

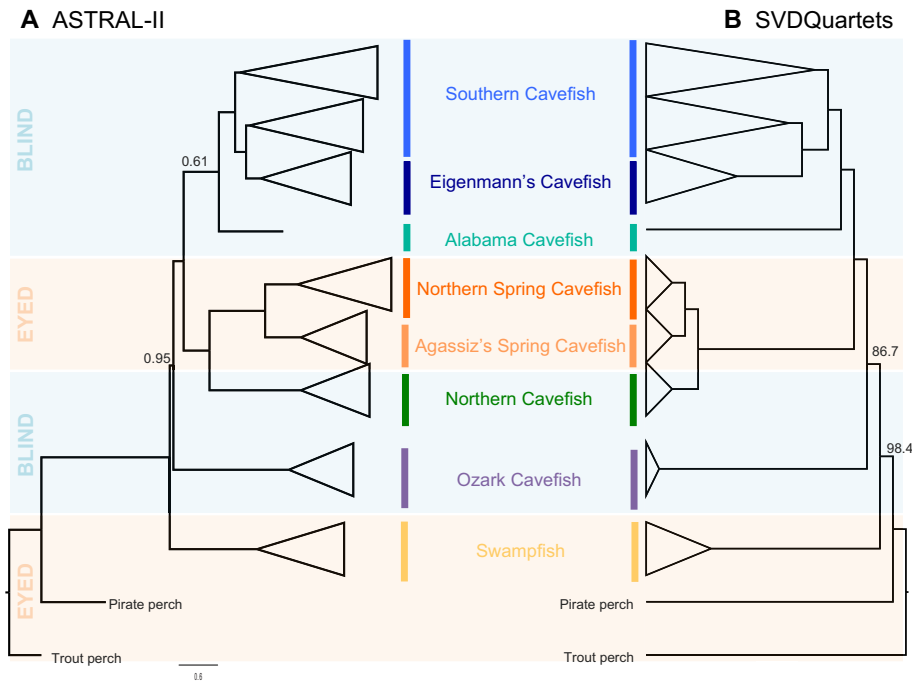


Figure 4. Phylogenetic relationships among the Amblyopsidae based on (A) ASTRAL and (B) SVDQuartets coalescent species trees with 50% majority rule consensus for SVDQuartets. Colored boxes indicate the extant taxa eye-state. Lower posterior probability and bootstrap node values are 1 and 100 unless otherwise noted, respectively. Scale bars indicate expected number of substitutions.

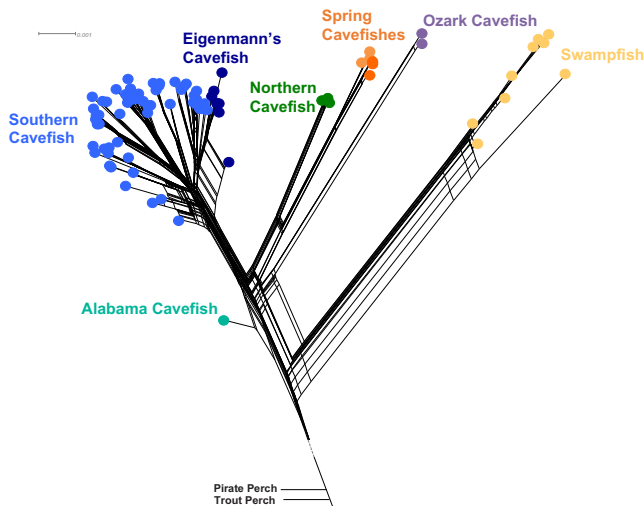


Figure 5. Splits network showing nontree-like relationships within the Amblyopsidae using distance estimates from sequences and Rooted Equal Angle algorithm for visualization.

respectively; Figs. S5B and S5C). In both the ARD and Irreversibility models, we found support for eyed ancestral states for the blind extant cavefishes (Figs. S5 and S5C, nodes I and II). Both Bayesian reconstruction and stochastic character mapping support multiple subterranean colonization events by an eyed ancestor.

GEOMETRIC MORPHOMETRICS

Full GM dataset

We found that the major axes of shape variation explained differences in head length to predorsal length ratio and body depth through PCA visualization (PC1 and PC2, respectively; Figs. 7A and S6). PC1 explained 44% and PC2 explained 13.77% of all shape variation. The blind cavefishes tended to have more elongate heads (negative PC1 scores) and slimmer bodies (negative PC2 scores), whereas the eyed Agassiz's Spring Cavefish and Swampfish had deeper bodies and shorter head length to predorsal length ratios (positive PC1 and PC2 scores). There were significant differences in shape between eye-states ($P = 0.001$ and $F = 33.41$).

GM data subset

In the reduced voucher dataset ($N = 18$), the eye-states differentiate along the first PC but do not appear to differentiate along PC2 (Figs. 7B and S7). We found that closely related species/populations tended to have similar body shapes ($K = 0.91$ and $P = 0.001$), but that eye-states have significantly different body shapes while accounting for phylogeny ($P = 0.05$ and $R^2 = 0.12$). There was no significant difference in the observed rates of morphological evolution for blind and eyed fishes (observed rate ratio = 1.15 and $P = 0.67$). Last, the independent cavefish lineages converged on similar body shapes (C1 = 0.17, $P = 0.001$; C2 = 0.014, $P = 0.001$).

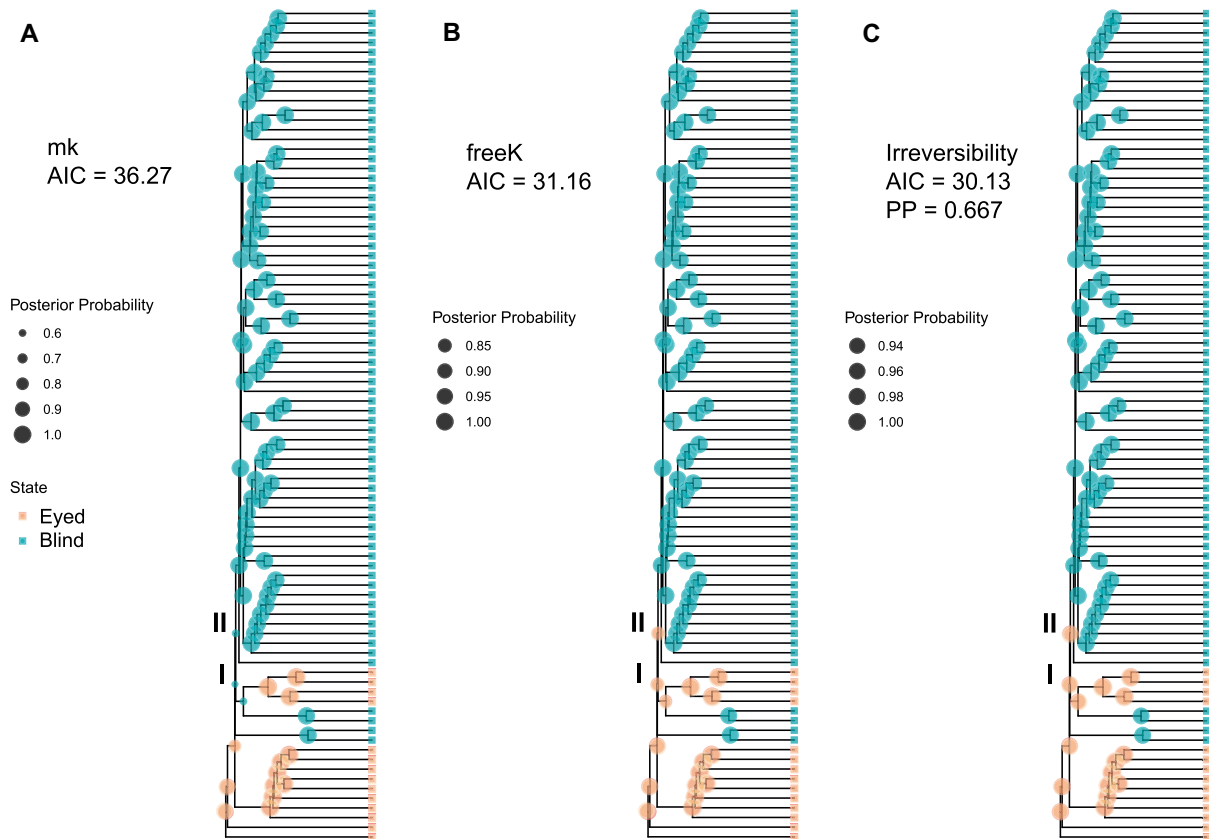


Figure 6. Ancestral eye-state reconstruction using Bayesian inference on the amblyopsid ASTRAL multispecies coalescent tree. Nodes referenced in text are numbered with roman numerals (I and II).

Discussion

The convergent loss of complex traits can occur in extreme environments that impose harsh selection pressures such as caves (Trontelj et al. 2012; Soares and Niemiller 2020). Whether these traits are lost forever remains an important topic in evolutionary biology (reviewed by Porter and Crandall 2003 and Collin and Miglietta 2008). Recent character state reconstructions have renewed the interest in ir/reversibility and have provided evidence for complex trait redevelopment or re-evolution (e.g., Collin and Cipriani 2003; Bonett et al. 2013). We demonstrate that North American cavefishes independently lost their eyes during cave adaptation multiple times and these lineages converged on similar cave-adapted body shapes.

EVOLUTIONARY RELATIONSHIPS OF THE AMBLYOPSIDAE

Most of our phylogenomic reconstructions (ASTRAL-II and SVDQuartets) are consistent with the phylogeny of Niemiller et al. (2013). We recovered the eyed spring cavefishes (*Forbesichthys* spp.) as the sister group to the blind Northern Cavefish, and the eyed Swampfish as the sister taxa to the rest of the family (Figs. 3 and 4). Interestingly, our ML

phylogeny presents a novel phylogenomic hypothesis where both the eyed Swampfish (*Chologaster cornuta*) and the eyed spring cavefishes (*Forbesichthys* spp.) are sister species to blind cavefishes.

The sister relationship we recover between the eyed spring cavefishes and the Northern Cavefish could be due to past introgression following hybridization as there is some syntopy in their range in the Mammoth Cave region (Fig. 2). There is evidence of nontree-like relationships within the amblyopsids between the blind Northern Cavefish and eyed spring cavefishes as well as between the blind Ozark Cavefish and eyed Swampfish with our splits network (Fig. 5). The blind Ozark Cavefish is found in the central part of the continental United States and the eyed Swampfish is found along the Atlantic coast of the United States (Fig. 2). The nonbifurcating relationships between these fishes could be due to incomplete lineage sorting or ancestral polymorphism rather than interbreeding or introgression. It is more likely that the sympatric blind Northern Cavefish and eyed spring cavefishes could have hybridized in the course of their evolutionary history. The nontree-like relationships indicate that the evolutionary history of sympatric blind and eyed amblyopsid fishes is complex and further studies examining the type of reticulation events are warranted.

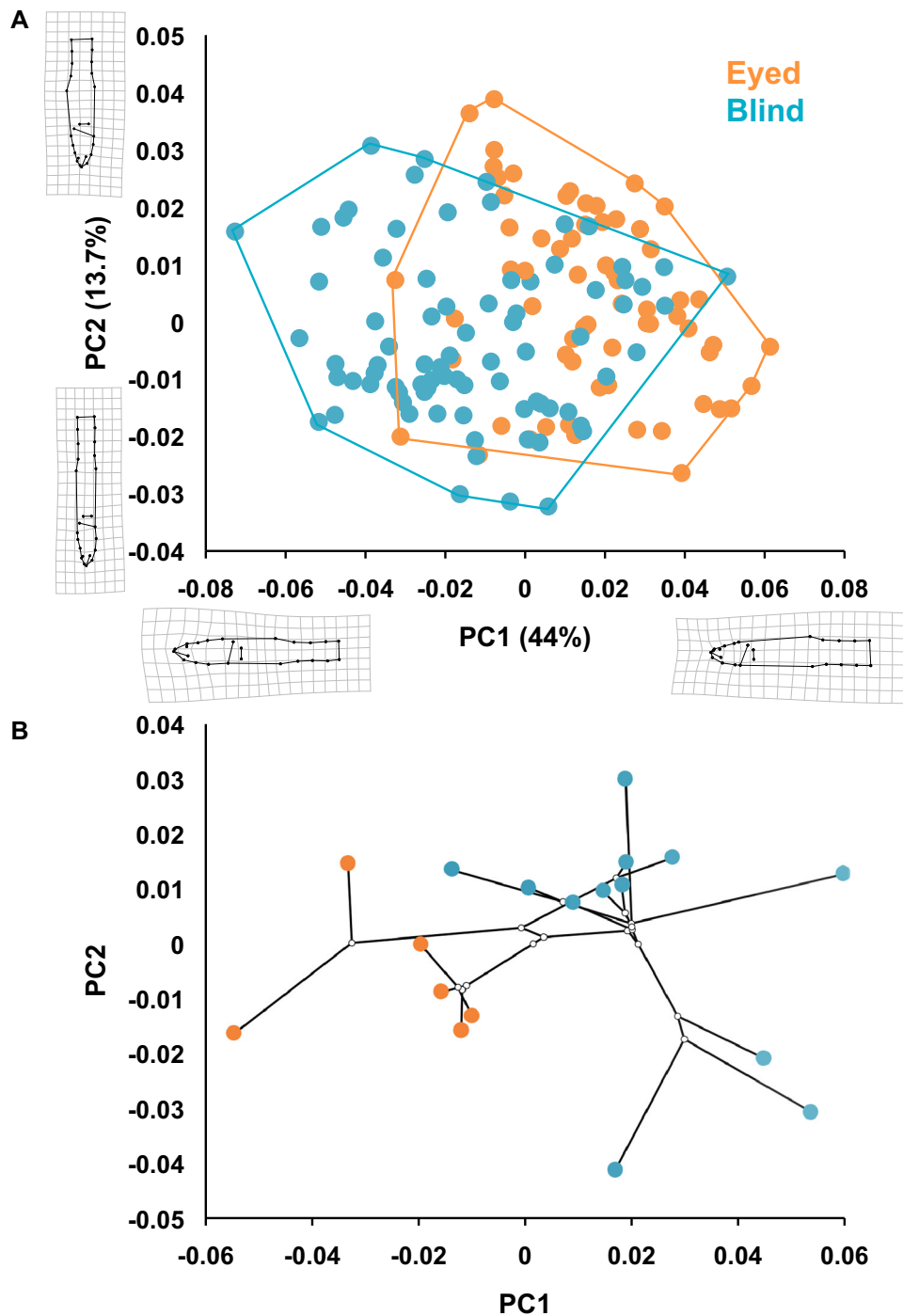


Figure 7. Geometric morphometric biplots for the Amblyopsidae fishes. PC1 is located on the X-axis and PC2 is located on the Y-axis. (A) Biplot of PC scores per individual for the full GM dataset ($N = 146$) colored by eye-state. Warp grids indicate the shape of the minimum and maximum specimen along that axis. (B) GM phylomorphospace of the amblyopsid data subset ($N = 18$) colored by eye-state.

DO THE EYES HAVE IT?

Our results are consistent with multiple, independent colonization events into the subterranean habitat followed by cave-adaptive convergent evolution (Figs. 6 and S5). Most previous molecular and morphological work also suggests multiple

subterranean invasions. Niemiller et al. (2013) found that cavefishes accrued mutations differently in the *rhodopsin* eye genes, suggesting a different mechanism for loss in each lineage. Additionally, Eigenmann (1909) found different lost eye characteristics in the cave-adapted amblyopsid lineages (e.g., extrinsic eye

muscles, rods and cones, and the vitreous chamber). However, Niemiller et al. (2013) performed model testing on their phylogenetic hypothesis and found the best support for an eye re-evolution scenario, where the spring cavefishes recolonized the surface from a common cavefish ancestor.

The amblyopsid ancestral state reconstructions highlight an interesting discussion about the loss and subsequent regaining of complex characteristics. Dollo's Law of Irreversibility has previously been challenged by other ancestral reconstructions and although our analyses support convergence (i.e., multiple subterranean invasions) over progressive regressionism or eye re-evolution in the eyed spring cavefishes, the possibility of eye reversibility is still intriguing. To break Dollo's Law, the molecular machinery behind the complex character must be lost and then regained (Collin and Miglietta 2008). Examining the genomes and transcriptomes of amblyopsid cavefishes would potentially lead to determination if the genetic changes that have led to eye loss are the same or different in cave species.

Our study provides a compelling case for the lack of progressive regressionism of eye characters (Woods and Inger 1957; Romero and Green 2005). We recognize that ancestral state reconstruction on only extant taxa may not be the full picture of the evolutionary history; however, there are currently no amblyopsid fossils to include in our analyses. Fossils would probably not tell us much because osteological characteristics of the orbits do not vary significantly between species of amblyopsids (authors pers. obs.), and it is unlikely to ever recover evidence of soft eye tissue from long extinct species.

AMBLYOPSID SHAPE EVOLUTION

Caves differ from terrestrial environments in several biotic and abiotic aspects that we expect could drive divergent patterns of morphological evolution. In addition to limited light availability, caves are often nutrient limited (Venarsky et al. 2014) and have relatively simple food webs that are dependent on periodic terrestrial subsidies (Simon et al. 2003; Roach et al. 2011). Additionally, conductivity tends to be lower in cave water, which can cause a heat shock like response in fishes (Rohner et al. 2013). All of these factors result in environmental stress that could place added selective pressure on efficient foraging, metabolism, and sensory perception—all aspects of cavefish biology possibly linked to variation in body shape. The different selective regimes imposed by cave and surface environments have resulted in different body shapes, but not different rates of body shape evolution.

We found the main shape differences between eyed and blind fishes to be head elongation (i.e., head length to predorsal length ratio), body depth, and head depth (Fig. 7). The cavefishes had long, slim heads and bodies, whereas the spring cavefishes and Swampfish had shorter heads and deeper heads and bodies. There is considerable body shape disparity within cavefishes, including

some body shapes found in surface forms (e.g., rounder, shorter heads). Despite there being more species richness in the cave-obligate amblyopsids and more morphological disparity in blind cavefishes, rates of body shape evolution did not differ between cave and surface environments. Caves have seemingly not led to a burst in diversification via novel ecological opportunity (Schluter 2000), perhaps because cave environments are simply too harsh to accommodate such a pattern (Venarsky et al. 2014).

CONVERGENT CAVE-ADAPTIVE EVOLUTION ACROSS TAXA

Next Generation Sequencing and phylogenomic studies have been able to clarify relationships among cave-obligate fishes and progress our knowledge of modes of subterranean adaptation (e.g., Phillips et al. 2017; Hedin et al. 2018). In Coghill et al. (2014), phylogeographic investigation with Single Nucleotide Polymorphisms and ancestral character state estimates show that the model Mexican Blind Cave Tetra (*Astyanax mexicanus*) have at least four independent origins of cave populations from surface ancestors. Additionally, phylogenomic reconstruction of three *Sinocyclocheilus* cyprinid fishes in Yang et al. (2016) shows a sister relationship between the surface *S. grahami* and the cave *S. anshuiensis* with the facultative cave-dwelling *S. rhinoceros* as the sister group to that clade; these relationships refute a hypothesis of progressive regression. Cave-dwelling brittle sea stars also have multiple independent colonization events into anchialine subterranean habitats (Bribiesca-Contreras et al. 2019). With the addition of our study on amblyopsids, we find further support for convergence and against progressive regression in cavefishes. The aforementioned studies show vastly different modes of subterranean adaptation among and within animal orders, varying in the number of transitions to cave environments, and sequence of adaptation.

Conclusions

Our phylogenetic investigations and ancestral state reconstructions suggested multiple independent cave colonization events within a single fish family; with this research, we have added additional support for multiple eye-loss events in cave taxa rather than progressive regressionism or eye redevelopment. Through examining shape variation between the eyed and blind amblyopsids, we showed that cave-adaptive evolution does have an effect on the body plan of fishes. Additionally, we found and quantified morphological convergence among independent cave lineages. By examining the evolutionary relationships, ancestral state, and shape evolution of the amblyopsids, we have brought a little more light to the many ways cave-obligate animals have adapted to an ecologically and physiologically demanding environment.

AUTHOR CONTRIBUTIONS

PBH performed the specimen collection, molecular lab work, phylogenetic reconstruction, GM data collection and processing, and manuscript writing. MLN performed the majority of specimen collection. EDB performed ancestral state reconstruction and reversibility testing. JWA performed specimen collection. WBL performed molecular lab work. PC performed specimen collection. All authors contributed to intellectual merit and manuscript writing.

ACKNOWLEDGMENTS

We would like to acknowledge the following for their assistance with this project: F. Alda for Ultraconserved Elements labwork and bioinformatics assistance; Z. Rodriguez, G. Mount, J. Storer, and J. Brown for computational assistance; C. D. R. Stephen, B. R. Kuhajda, and T. Fobian for tissue specimen collection assistance; S. Friedman for geometric morphometrics analysis assistance; and The Chakrabarty Lab including D. Elias, L. Morgan, and A. Turner for intellectual support. Our funding sources include the Society of Systematic Biologists Graduate Student Research award, the Systematics Research Fund from the Systematics Association and the Linnean Society, and the Sigma Xi Honor Society Grants in Aid of Research award to PBH and National Science Foundation 1839915 to PC.

DATA ARCHIVING

Raw sequence data are archived in the NCBI Sequence Repository Archive (PRJ610650). Concatenated gene alignments are archived on Dryad with Supplementary Materials (<https://doi.org/10.5061/dryad.crjdfn31m>). Molecular and morphological specimens accession numbers are available in the Supplementary Material.

CONFLICT OF INTEREST

The authors declare no conflict of interest.

LITERATURE CITED

- Adams, D. C. 2014a. A generalized K statistic for estimating phylogenetic signal from shape and other high-dimensional multivariate data. *Syst. Biol.* 63:685–697. <https://doi.org/10.1093/sysbio/syu030>
- Adams, D. C. 2014b. Quantifying and comparing phylogenetic evolutionary rates for shape and other high-dimensional phenotypic data. *Syst. Biol.* 63:166–177.
- Adams, D. C., and E. Otárola-Castillo. 2013. geomorph: an R package for the collection and analysis of geometric morphometric shape data. *Methods Ecol. Evol.* 4:393–399. <https://doi.org/10.1111/2041-210X.12035>
- Adams, D. C., and M. L. Collyer. 2018. Multivariate phylogenetic comparative methods: evaluations, comparisons, and recommendations. *Syst. Biol.* 67:14–31.
- Adams, D., M. Collyer, and A. Kaliontzopoulou. 2019. Geomorph: Software for geometric morphometric analyses. R package version 3.1.0. Available via <https://cran.r-project.org/package=geomorph>.
- Agassiz, J. L. R. 1853. Recent researches of Prof. Agassiz. *Am. J. Sci. Arts* 16:134.
- Alter, S. E., B. Brown, and M. L. J. Stiassny. 2015. Molecular phylogenetics reveals convergent evolution in lower Congo River spiny eels. *BMC Evol. Biol.* 15:224. <https://doi.org/10.1186/s12862-015-0507-x>
- Armbruster, J. W., M. L. Niemiller, and P. B. Hart. 2016. Morphological evolution of the cave-, spring- and swampfishes of the Amblyopsidae (Percopsiformes). *Copeia* 104:763–777.
- Azua-Bustos, A., C. González-Silva, C. Arenas-Fajardo, and R. Vicuña. 2012. Extreme environments as potential drivers of convergent evolution by exaptation: the Atacama Desert Coastal Range case. *Front. Microbiol.* 3:1–9. <https://doi.org/10.3389/fmicb.2012.0042>
- Bergsten, J. 2005. Review of long-branch attraction. *Cladistics* 21:163–193.
- Berta, A., J. L. Sumich, and K. M. Kovacs. 2006. Marine mammals: evolutionary biology. Academic Press, Cambridge, MA.
- Betancur-R., R., R. E. Broughton, E. O. Wiley, K. Carpenter, J. A. López, C. Li, N. I. Holcroft, D. Arcila, M. Sanciangco, J. C. Li Cureton, et al. 2013. The Tree of Life and a new classification of bony fishes. *PLoS Curr.* <https://doi.org/10.1371/currents.tol.53ba26640df0cace75bb165c8c26288>
- Blomberg, S. P., T. Garland JR., and A. R. Ives. 2003. Testing for phylogenetic signal in comparative data: behavioral traits are more labile. *Evolution* 57:717–745.
- Bolger, A. M., M. Lohse, and B. Usadel. 2014. Trimmomatic: a flexible trimmer for Illumina sequence data. *Bioinformatics* 30:2114–2120. <https://doi.org/10.1093/bioinformatics/btu170>
- Bollback, J. P. 2006. SIMMAP: stochastic character mapping of discrete traits on phylogenies. *BMC Bioinformatics* 7:1–7. <https://doi.org/10.1186/1471-2105-7-88>
- Bonett, R. M., M. A. Steffen, S. M. Lambert, J. J. Wiens, and P. T. Chippindale. 2013. Evolution of paedomorphosis in plethodontid salamanders: ecological correlates and re-evolution of metamorphosis. *Evolution* 68:466–482. <https://doi.org/10.1111/evo.12274>
- Bribiesca-Contreras, G., T. Pineda-Enríquez, F. Márquez-Borrás, F. A. Solís-Marín, H. Verbruggen, A. F. Hugall, and T. D. O'Hara. 2019. Dark offshoot: phylogenomic data sheds light on the evolutionary history of a new species of cave brittle star. *Mol. Phylogenet. Evol.* 136:151–163. <https://doi.org/10.1016/j.ympev.2019.04.014>
- Burruss, P. B. H., E. D. Burruss, and J. W. Armbruster. 2017. Body shape variation within the Southern Cavefish, *Typhlichthys subterraneus* (Percopsiformes: Amblyopsidae). *Zoomorphology* 136:365–377. <https://doi.org/10.1007/s00435-017-0360-0>
- Chakrabarty, P., J. A. Prejean, and M. L. Niemiller. 2014. The Hoosier cavefish, a new and endangered species (Amblyopsidae, Amblyopsis) from the caves of southern Indiana. *ZooKeys* 412:41–57. <https://doi.org/10.3897/zookeys.412.7245>
- Charlton, H. H. 1933. The optic tectum and its related fiber tracts in blind fishes. A. *Troglichthys rosae* and *Typhlichthys eigenmanni*. *J. Comp. Neurol.* 57:285–325.
- Chifman, J., and L. Kubatko. 2014. Quartet inference from SNP data under the coalescent. *Bioinformatics* 30:3317–3324.
- Christiansen, K. 2012. Morphological adaptations. Pp. 517–528 in W. B. White and D. C. Culver, eds. *Encyclopedia of caves*, 2nd ed. Elsevier Academic Press, Amsterdam, the Netherlands.
- Coghill, L. M., C. D. Hulsey, J. Chaves-Campos, F. J. García de Leon, and S. G. Johnson. 2014. Next generation phylogeography of cave and surface *Astyanax mexicanus*. *Mol. Phylogenet. Evol.* 79:368–374. <http://doi.org/10.1016/j.ympev.2014.06.029>
- Collin, R., and M. P. Miglietta. 2008. Reversing opinions on Dollo's Law. *Trends Ecol. Evol.* 23:602–609. <https://doi.org/10.1016/j.tree.2008.06.013>
- Collin, R., and R. Cipriani. 2003. Dollo's law and the re-evolution of shell coiling. *Proc. R. Soc. B* 270:2551–2555. <https://doi.org/10.1098/rspb.2003.2517>
- Conway Morris, S. 2010. Evolution: like any other science it is predictable. *Philos. Trans. R. Soc. B* 365:133–145.
- Cooper, J. E., and R. A. Kuehne. 1974. *Speoplatyrhinus poulsoni*, a new genus and species of subterranean fish from Alabama. *Copeia* 1974:486–493.
- DeKay, J. E. 1842. Zoology of New York or the New York fauna; comprising detailed descriptions of all the animals hitherto observed within the

- state of New York with brief notices of those occasionally found near its borders, and accompanied by appropriate illustrations. Part IV. W. and A. White and J. Visscher, Albany, NY.
- Denton, J. S. S., and D. C. Adams. 2015. A new phylogenetic test for comparing multiple high-dimensional evolutionary rates suggests interplay of evolutionary rates and modularity in lanternfishes (Myctophiformes; Myctophidae). *Evolution* 69:2425–2440.
- Dillman, C. B., D. E. Bergstrom, D. B. Noltie, T. P. Holtsford, and R. L. Mayden. 2011. Regressive progression, progressive regression or neither? Phylogeny and evolution of the Percopsiformes (Teleostei, Paracanthopterygii). *Zool. Sci.* 40:45–60.
- Dollo, L. 1893. Les lois de l'évolution. *Bull. Soc. Belge. Geol. Pal. Hydr.* VII:164–166.
- Domes, K., R. A. Norton, M. Maraun, and S. Scheu. 2007. Reevolution of sexuality breaks Dollo's law. *Proc. Natl. Acad. Sci.* 104:7139–7144. <https://doi.org/10.1073/pnas.0700034104>
- Edgington, H. A., and D. R. Taylor. 2019. Ecological contributions to body shape evolution in salamanders of the genus *Eurycea* (Plethodontidae). *PLoS ONE* 14:1–14. <https://doi.org/10.1371/journal.pone.0216754>
- Eigenmann, C. H. 1897. The Amblyopsidae, the blind fish of America. Report Brit. Assoc. Adv. Sci. 1897:685–686.
- . 1898. A new blind fish. *Proc. Indiana Acad. Sci.* 1897:231.
- . 1909. Cave vertebrates of America: a study in degenerative evolution. Carnegie Institution of Washington, Washington, DC.
- Faircloth, B. C., J. E. McCormack, N. G. Crawford, M. G. Harvey, R. T. Brumfield, and T. C. Glenn. 2012. Ultraconserved elements anchor thousands of genetic markers spanning multiple evolutionary timescales. *Syst. Biol.* 61:717–726.
- Faircloth, B. C., L. Sorenson, F. Santini, and M. E. Alfaro. 2013. Phylogenomics perspective on radiation of ray-finned fishes based upon targeted sequencing of Ultraconserved Elements (UCEs). *PLoS ONE* 8:e65923. <https://doi.org/10.1371/journal.pone.0065923>
- Faircloth, B. C. 2016. PHYLUCE is a software package for the analysis of conserved genomic loci. *Bioinformatics* 32:786–788. <https://doi.org/10.1093/bioinformatics/btv646>
- Felsenstein, J. 1978. Cases in which parsimony or compatibility methods will be positively misleading. *Syst. Biol.* 27:401–410. <https://doi.org/10.1093/sysbio/27.4.401>
- Fenolio, D. B., M. L. Niemiller, M. G. Levy, and B. Martinez. 2013. Conservation status of the Georgia Blind Salamander (*Eurycea wallacei*) from the Floridian Aquifer of Florida and Georgia. *IRCF Reptiles Amphib.* 20:97–111.
- Forbes, S. A. 1882. The blind cave fishes and their allies. *Am. Nat.* 16:1–5.
- Gambette, P., and D. H. Huson. 2008. Improved layout of phylogenetic networks. *IEE/ACM Trans. Comput. Biol. Bioinform.* 5:1–8.
- Girard, C. F. 1859. Ichthyological notices. *Proc. Acad. Nat. Sci. Philadelphia* 1859:56–68.
- Goldberg, E. E., and B. Igić. 2008. On phylogenetic tests of irreversible evolution. *Evolution* 62:2727–2741.
- Gower, J. C. 1975. Generalized Procrustes analysis. *Psychometrika* 40:33–51.
- Hedin, M., and S. M. Thomas. 2009. Molecular systematics of eastern North American Phalangodidae (Arachnida: Opiliones: Laniatores), demonstrating convergent morphological evolution in caves. *Mol. Phylogenet. Evol.* 54:107–121. <https://doi.org/10.1016/j.ympev.2009.08.020>
- Hedin, M., S. Derkarabetian, J. Blair, and P. Paquin. 2018. Sequence capture phylogenomics of eyeless *Cicurina* spiders from Texas caves with emphasis on US federally-endangered species from Bexar County (Araneae, Hahniidae). *ZooKeys* 769:49–76. <https://doi.org/10.3897/zookeys.769.25814>
- Höhna, S., M. J. Lands, T. A. Heath, B. Boussau, N. Lartillot, B. R. Moore, J. P. Huelsenbeck, and F. Ronquist. 2016. RevBayes: Bayesian phylogenetic inference using graphical models and an interactive model-specification language. *Syst. Biol.* 65:726–736. <https://doi.org/10.1093/sysbio/syw021>
- Huelsenbeck, J. P. 1997. Is the Felsenstein zone a fly trap? *Syst. Biol.* 46:69–74.
- Huson, D. H., and D. Bryant. 2006. Application of phylogenetic networks in evolutionary studies. *Mol. Biol. Evol.* 23:254–267.
- Huson, D. H., and C. Scornavacca. 2011. A survey of combinatorial methods for phylogenetic networks. *Genome Biol. Evol.* 3:23–35.
- Klingenberg, C. P. 2016. Size, shape, and form: concepts of allometry in geometric morphometrics. *Dev. Genes Evol.* 226:113–137. <https://doi.org/10.1007/s00427-016-0539-2>
- Lanfear, R., P. B. Frandsen, A. M. Wright, T. Senfeld, and B. Calcott. 2017. PartitionFinder 2: new methods for selecting partitioned models of evolution formolecular and morphological phylogenetic analyses. *Mol. Biol. Evol.* 34:772–773. <https://doi.org/10.1093/molbev/msw260>
- Losos, J. B. 2011. Convergence, adaptation, and constraint. *Evolution* 65:1827–1840. <https://doi.org/10.1111/j.1558-5646.2011.01289.x>
- Lynch, V. J., and G. P. Wagner. 2009. Did egg-laying boas break Dollo's law? Phylogenetic evidence for reversal to oviparity in Sand Boas (*Eryx*: Boidae). *Evolution* 64:207–216. <https://doi.org/10.1111/j.1558-5646.2009.00790.x>
- Martinez, Q., R. Lebrun, A. S. Achmadi, J. A. Esselstyn, A. R. Evans, L. R. Heaney, R. P. Miquez, K. C. Rowe, and P. H. Fabre. 2018. Convergent evolution of an extreme dietary specialization, the olfactory system of worm-eating rodents. *Sci. Rep.* 8:17806. <https://doi.org/10.1038/s41598-018-35827-0>
- McGee, M. D., B. C. Faircloth, S. R. Borstein, J. Zheng, C. Darrin Hulsey, P. C. Wainwright, and M. E. Alfaro. 2016. Replicated divergence in cichlid radiations mirrors a major vertebrate innovation. *Proc. Royal Soc. B* 283:20151413.
- Mirarab, S., and T. Warnow. 2015. ASTRAL-II: coalescent-based species tree estimation with many hundreds of taxa and thousands of genes. *Bioinformatics* 12:i44–i52. <https://doi.org/10.1093/bioinformatics/btv234>
- Morrison, D. 2011. An introduction to phylogenetic networks. RJR Productions, Uppsala, Sweden.
- Near, T. J., R. I. Eytan, A. Dornburg, K. L. Kuhn, J. A. Moore, M. P. Davis, P. C. Wainwright, M. Friedman, and W. L. Smith. 2012. Resolution of ray-finned fish phylogeny and timing of diversification. *Proc. Natl. Acad. Sci. USA* 109:13698–13703.
- Niemiller, M. L., and T. M. Poulson. 2010. Subterranean fishes of North America. Pp. 168–280 in E. Trajano, M. E. Bichuette, and B. G. Kapoor, eds. *Biology of subterranean fishes*, CRC Press, Boca Raton, FL.
- Niemiller, M. L., T. J. Near, and B. M. Fitzpatrick. 2012. Delimiting species using multilocus data: diagnosing cryptic diversity in the Southern Cavefish, *Typhlichthys subterraneus* (Teleostei: Amblyopsidae). *Evolution* 66:846–866.
- Niemiller, M. L., B. M. Fitzpatrick, P. Shah, L. Schmitz, and T. J. Near. 2013. Evidence for repeated loss of selective constraint in rhodopsin of amblyopsid cavefishes (Teleostei: Amblyopsidae). *Evolution* 67:732–748.
- Niemiller, M. L., K. S. Zigler, P. B. Hart, B. R. Kuhajda, J. W. Armbruster, B. N. Ayala, and A. S. Engel. 2016. First definitive record of a stygobiotic fish (Percopsiformes, Amblyopsidae, *Typhlichthys*) from the Appalachian karst region in the eastern United States. *Subterr. Biol.* 20:39–50.
- Oakley, T. H., and C. W. Cunningham. 2002. Molecular phylogenetic evidence for the independent evolutionary origin of an arthropod compound eye. *Proc. Natl. Acad. Sci.* 99:1426–1430. www.pnas.org/cgi/doi/10.1073.pnas.032483599

- Page, C. E., and N. Cooper. 2017. Morphological convergence in 'river dolphin' skulls. *PeerJ* 5:e4090. <https://doi.org/10.7717/peerj.4090>
- Paradis, E., J. Claude, and K. Strimmer. 2004. APE: analyses of phylogenetics and evolution in R language. *Bioinformatics* 20:289–290. <https://doi.org/10.1093/bioinformatics/btg412>
- Porter, M. L., and K. A. Crandall. 2003. Lost along the way: the significance of evolution in reverse. *Trends Ecol. Evol.* 18:541–547.
- Passow, C. N., R. Greenway, L. Arias-Rodriguez, P. D. Jeyasingh, and M. Tobler. 2015. Reduction of energetic demands through modification of body size and routine metabolic rates in extremophile fish. *Physiol. Biochem. Zool.* 88:371–383.
- Passow, C. N., L. Arias-Rodriguez, and M. Tobler. 2017. Convergent evolution of reduced energy demands in extremophile fish. *PLoS ONE* 12:e0186935. <https://doi.org/10.1371/journal.pone.0186935>
- Phillips, J. G., D. B. Fenolio, E. S.L., and R. M. Bonett. 2017. Hydrologic and geologic history of the Ozark Plateau drive phylogenomic patterns in a cave-obligate salamander. *J. Biogeogr.* 44:2463–2474. <https://doi.org/10.1111/jbi.13047>
- Pipán, T., and D. C. Culver. 2012. Convergence and divergence in the subterranean realm: a reassessment. *Biol. J. Linn. Soc.* 107:1–14.
- Poulson, T. L. 1963. Cave adaptation in amblyopsid fishes. *Am. Midl. Nat.* 70:257–291.
- Putnam, F. W. 1872. The blind fishes of the Mammoth Cave and their allies. *Am. Nat.* 6:6–30.
- Revell, L. J. 2012. phytools: an R package for phylogenetic comparative biology (and other things). *Methods Ecol. Evol.* 3:217–223. <https://doi.org/10.1111/j.2041-210X.2011.00169.x>
- Roach, K. A., M. Tobler, and K. O. Winemiller. 2011. Hydrogen sulfide, bacteria, and fish: a unique, subterranean food chain. *Ecology*. 92:2056–2062.
- Rohlf, F. J. 2010. tpsDig2 version 2.16. Department of Ecology and Evolution, State University of New York, Stony Brook, NY.
- Rohner, N., D. F. Jarosz, J. E. Kowalko, M. Yoshizawa, W. R. Jeffery, R. L. Borowsky, S. Lindquist, and C. J. Tabin. 2013. Cryptic variation in morphological evolution: HSP90 as a capacitor for loss of eyes in cavefish. *Science* 342:1372–1375.
- Romero, A., and S. M. Green. 2005. The end of regressive evolution: examining and interpreting the evidence from cave fishes. *J. Fish Biol.* 67:3–32.
- Schluter, D. 2000. The ecology of adaptive radiation. Oxford University Press, Oxford, U.K.
- Sidlauskas, B. 2008. Continuous and arrested morphological diversification in sister clades of characiform fishes: a phylomorphospace approach. *Evolution* 62:3135–3156. <https://doi.org/10.1111/j.1558-5646.2008.00519.x>
- Simon, K. S., E. F. Benfield, and S. A. Macko. 2003. Food web structure and the role of epilithic biofilms in cave streams. *Ecology* 84:2395–2406.
- Simpson, J. T., K. Wong, S. D. Jackman, J. E. Schein, S. J. M. Jones, and I. Birol. 2009. ABySS: a parallel assembler for short read sequence data. *Genome Res.* 19:1117–1123.
- Soares, D., and M. L. Niemiller. 2013. Sensory adaptations of fishes to subterranean environments. *Bioscience* 63:274–283.
- . 2020. Extreme adaptation in caves. *Anat. Rec.* 303:15–23. <https://doi.org/10.1002/ar.24044>
- Springer, V. G., and G. D. Johnson. 2004. Study of the dorsal gill-arch musculature of Teleostome fishes, with special reference to the Actinopterygii. *Bull. Biol. Soc. Wash.* 11:237–262.
- Stamatakis, A. 2014. RAxML version 8: a tool for phylogenetic analysis and post-analysis of large phylogenies. *Bioinformatics* 30:1312–1313.
- Stayton, C. T. 2015. The definition, recognition, and interpretation of convergent evolution and two new measures for quantifying and assessing the significance of convergence. *Evolution* 69:2140–2153. <https://doi.org/10.1111/evo.12729>
- Swofford, D. L. 2002. PAUP*: phylogenetic analysis using parsimony (*and other methods). Sinauer Associates, Sunderland, MA.
- Trontelj, P., A. Blejec, and C. Fišer. 2012. Ecomorphological convergence of cave communities. *Evolution* 66:3852–3865.
- Venarsky, M. P., B. M. Huntsman, A. D. Hurn, J. P. Benstead, and B. R. Kuhajda. 2014. Quantitative food web analysis supports the energy-limitation hypothesis in cave stream ecosystems. *Oecologia* 176:859–869.
- Woods, L. P., and R. F. Inger. 1957. The cave, spring, and swamp fishes of the family Amblyopsidae of Central and Eastern United States. *Am. Midl. Nat.* 58:232–256.
- Yang, J., X. Chen, J. Bai, D. Fang, Y. Qiu, W. Jiang, H. Yuan, C. Bian, J. Lu, S. He, et al. 2016. The *Sinocyclocheilus* cavefish genome provides insights into cave adaptation. *BMC Biol.* 14:1–14. <https://doi.org/10.1186/s12915-015-0223-4>

Associate Editor: A. Kaliontzopoulou
Handling Editor: T. Chapman

Supporting Information

Additional supporting information may be found online in the Supporting Information section at the end of the article.

Table S1. Tissue specimens used for the UCE dataset (N = 110).

Table S2. Museum specimens used in the full GM dataset (N = 146).

Table S3. Specimen identification for the GM subset (N = 18).

Fig. S1. Lateral GM landmark scheme for the amblyopsids based on Burress et al. (2017).

Fig. S2. Amblyopsid RAxML phylogenomic hypothesis with all individuals labeled.

Fig. S3. Amblyopsid ASTRAL-II coalescent species tree with all individuals labeled.

Fig. S4. Amblyopsid SVDQuartets consensus coalescent species tree with all individuals labeled.

Fig. S5. Summary of 1000 mapped character states using stochastic character mapping of eye-state.

Fig. S6. Biplots of PC scores per individual for the full GM dataset (N = 146) colored by species.

Fig. S7. GM Phylomorphospace of the amblyopsid data subset (N = 18) with species colored and ellipses surrounding the eye-states (blue = blind, orange = eyed).